Water Practice & Technology

IWA PUBLISHING

Water Practice & Technology Vol 19 No 3, 692 doi: 10.2166/wpt.2024.037

Harnessing the potential of zinc oxide nanoparticles from *Strychnos potatorum* seeds impregnated with activated carbon for an effective removal of fluoride in deep soil water

Akshaya V. and Jayanthi G.*

Department of Biochemistry PG & Research, Government Arts College for Women, Krishnagiri-635 002, TamilNadu, South India
*Corresponding author. E-mail: jayanthijr2011@gmail.com

AV, 0000-0002-8256-5376; JG, 0000-0002-7236-4714

ABSTRACT

Fluoride (F^-) contamination in global water sources is a growing concern, prompting the need for innovative solutions. This explores a novel method using zinc oxide nanoparticle-activated carbon (ZnO-NP/AC) composite for efficient fluoride removal from deep soil water, aiming to evaluate its effectiveness in attracting fluoride contaminants. The focus is on treatment of water sample collected from Dharmapuri, Tamil Nadu, using green synthesis method for ZnO-NP/AC column filter. Employed an exclusive column adsorption method, investigated on physiochemical parameters in water before and after running the column. Fluoride concentration and TDS where significantly harnessed in water after running the green synthesis composite column filter. Characterization of green synthesized nanoparticles of *Strychnos potatorum* seed powder synthesis with ZnO NPs. Green synthesis successes were confirmed in two ways; one way is UV-visible spectrophotometer technique in depth quantity peak and another one is graphically peak from SEM, density and crystalline structure in XRD techniques. Column composite with *S.potatorum* ZnO-AC NPs has removed fluoride efficiently (80.5%) at range of 20 g/L for a contact time of 60 minutes, surpassing World health organization (WHO) guidelines for safe drinking water. In conclusion ZnO-AC NPs composite is a sustainable and cost-effective method for effective removal of fluoride contaminants from deep soil water, addressing a pressing global issue.

Key words: contaminants, deep soil water, defluoridation, nanoadsorbent, nontoxicity, water purification

HIGHLIGHTS

- Sustainable and eco-friendly approach for synthesizing zinc oxide nanoparticles.
- Composite coating enhances activated carbon defluoridation capacity.
- Improved defluoridation efficiency was observed compared to conventional methods.
- Cost-effective and accessible solution for fluoride removal.
- Contribution to water quality improvement and reducing health risk.

GRAPHICAL ABSTRACT

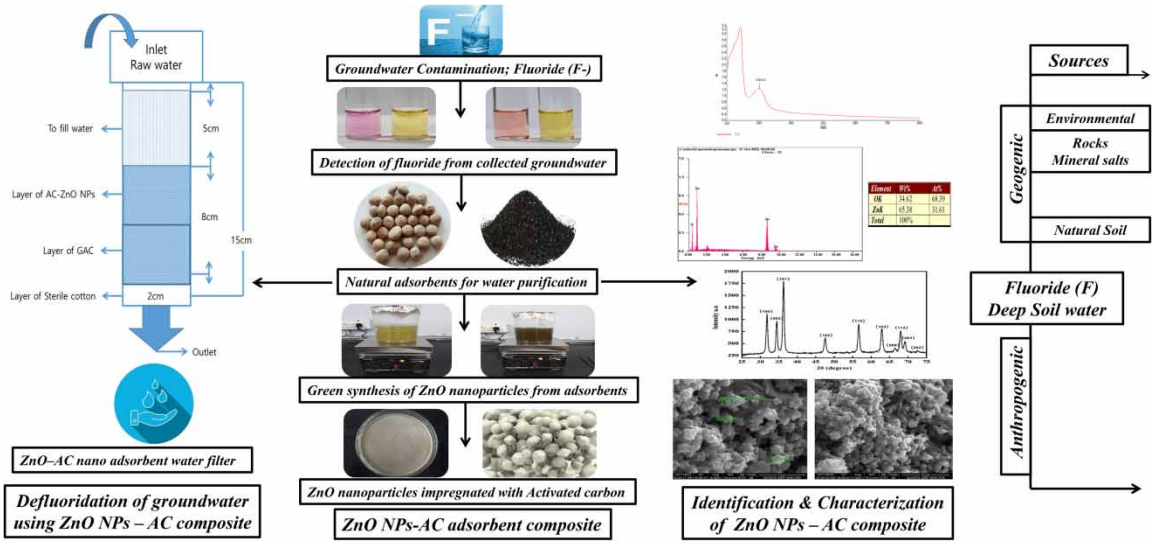

NOMENCLATURE

F^-	fluoride
ZnO	NP/AC – zinc oxide nanoparticles/activated carbon
SEM	scanning electron microscopy
HRSEM	high-resolution SEM
XRD	X-ray diffraction
EDX	energy-dispersive X-ray
WHO	World Health Organization
ICMR	Indian Council of Medical Research
BIS	Bureau of Indian Standards
GAC	granular activated carbon
SAIF	Sophisticated Analytical Instrumentation Facility Centre
APHA	American Public Health Association
L	Litre
TDS	total dissolved solids
TS	total solids
EC	electrical conductivity
TSS	total suspended solids
TWAD	Tamil Nadu Water Analyzing Department
SPR	surface plasmon resonance
JCPSD	Joint Committee on Powder Diffraction Standards
Ca^+	calcium
Mg^{2+}	magnesium
NaOH	sodium hydroxide
$CaCl_3$	calcium chloride
Zn	zinc
$Zn(NO_3)_2{\cdot}6H_2O$	zinc nitrate hexahydrate
GO	graphene oxide

1. INTRODUCTION

Safe drinking water is essential for human health and all-life well-being, but natural water is contaminated due to the interaction of the soil, rocks, industrialization, and urbanization. Contaminants such as fluoride, arsenic, iron, lead, cadmium, and other contaminants can be found in deep soil water (Elhalil *et al.* 2016). Fluoride (F^-) is a substance consumed by several million people worldwide and is currently claiming the lives of 200 million people across 25 countries (Rasool *et al.* 2018). According to Saxena & Sewak's (2015) findings, 17 out of India's 25 states – including Rajasthan, Andhra Pradesh, Tamil Nadu, Gujarat, and Uttar Pradesh – and approximately 10 million people are found to be affected by local fluorosis. The optimal fluoride concentration in

drinking water is between 0.5 and 1.0 mg/l, according to recommendations from the WHO (Ahmad *et al.* 2022). Excessive fluoride concentrations in drinking water can lead to negative health consequences, such as dental fluorosis, skeletal fluorosis, and disorders of the brain (Kashyap *et al.* 2021).

Fluoride levels in drinking water have been observed to be high in various geographical areas in Dharmapuri, Tamil Nadu, India. The WHO and Bureau of Indian Standards (BIS) established a range of permissible fluoride concentrations in drinking water for a particular location based on climatic circumstances because the amount of water drunk, and hence the amount of fluoride ingested, is mostly controlled by air temperature (Joshua Amarnath *et al.* 2015). Numerous clinical and laboratory investigations have demonstrated that F^- modifies the morphology and biochemistry of the brain, resulting in an individual's neurological development, as highlighted by Ren *et al.* (2022) in their review of these findings. Identifying this issue and identifying potential solutions are among the most important issues associated with defluoridation. To remove fluoride via inorganic approaches, numerous tried-and-true techniques have been developed (Singh *et al.* 2016).

Numerous techniques, including ion exchange, membrane separation, precipitation–coprecipitation, adsorption, chemical coagulation, etc. are employed to remove fluoride. Due to its low cost, environmental friendliness, practical use, and use of toxic sludge, adsorption is a commonly used fluoride removal method (Joshi *et al.* 2020). Adsorbents such as hydroxyapatite (Maity *et al.* 2018), zirconium-impregnated activated carbon (AC) (Sonal *et al.* 2020), cerium dioxide (Rashid *et al.* 2021), and zinc magnesium aluminium ternary oxides have been established for defluoridation but have disadvantages such as low adsorption capacity and long equilibrium time (Gao *et al.* 2020). Due to their unique characteristics and potential uses in water treatment and purification systems, nanoparticles (NPs) have attracted much attention (Mahvi *et al.* 2019; Al-Hazmi *et al.* 2024).

The preparation of highly effective, economical, and environmental friendly adsorbents is desirable. Due to its affordability, nontoxicity, and structural stability, ZnO is a fascinating material for the treatment of water. Zinc oxide nanoparticles (ZnO NPs) possess several desirable characteristics, such as high adsorption efficiency, large surface area, and high surface reactivity (Bazrafshan *et al.* 2016). AC is an effective adsorbent for water treatment due to its high porosity and large surface area. However, its adsorption capacity for fluoride is limited, necessitating the development of novel composite materials to enhance its fluoride removal efficiency (Naga *et al.* 2022).

Nanoscale materials have become popular water treatment materials due to their physicochemical characteristics, such as a larger surface area, increased reactivity, and self-assembly (Kumar 2023). Nanostructured metal oxide particles have a higher sorption capacity due to their surface adsorption sites. Only a few reports have been published on the use of nanoscale metal oxides to remove fluoride and other anions from water (Lu *et al.* 2023).

The present study aimed to investigate the feasibility of using a composite material consisting of green-synthesized ZnO NPs coated on AC for deep soil water defluoridation. This study assessed the viability and potential of nanosized ZnO impregnated with AC (ZnO NPs-AC) for water purification and defluoridation and the characterization of ZnO NPs-AC using high-resolution scanning electron microscopy (HRSEM), X-ray diffraction (XRD), and energy-dispersive X-ray (EDX) analysis. The composite material will be synthesized using a simple, cost-effective, and environmentally friendly method, ensuring its potential for large-scale implementation.

2. METHODS

2.1. Reagents and chemicals

Analytical-grade chemicals and reagents were all employed in the experiment without further purification. Sigma Aldrich, USA, provided zinc nitrate hexahydrate ($Zn(NO_3)_2{\cdot}6H_2O$; 98% purity). All reagents used were of analytical grade and obtained from Merck (Germany): sodium hydroxide, NaOH (98% purity); calcium chloride, $CaCl_3$, and hydrochloric acid; and HCl (99% purity). All the solutions were made with deionized water.

2.2. Collection of sample materials

Strychnos potatorum seed powder was collected from the Agasthiyar herbal products shop in K. pudhur, Madurai. The deep soil water samples were collected from Dharmapuri districts in Tamil Nadu, India. The water samples were analyzed to determine the fluoride content, and the collected samples were subjected to further analysis.

2.3. Geographical zone and sample site location

The study area of the Dharmapuri district, Tamil Nadu, is known for its agricultural activities and diverse topography. However, one concerning issue in this region is the prevalence of fluoride in the water sources. Fluoride contamination is a significant problem affecting many parts of Dharmapuri districts, including the village of Pappireddipatti. Pappireddipatti village is located in the northern part of Dharmapuri district and has been grappling with high fluoride levels in their water sources. This issue has serious implications for the health and well-being of the local population. The sampling sites were Pappireddipatti (approximately 12.1144°N longitude and 78.1819°E longitude), and researchers can gather valuable data on the fluoride levels in the water. This includes analyzing fluoride concentration, pH levels, and other parameters associated with water quality.

2.4. Preparation of plant extract

About 50 g of *S. potatorum* seed powder was weighed and collected for analysis. The extract was prepared by taking 50 g in 200 ml, placing it into a 400 ml beaker, stirring for 2 hours at room temperature, and leaving it overnight. The extract was subsequently filtered and used for NP synthesis (Prabhu *et al.* 2014).

2.5. Preparation of ZnO NPs by a green synthesis method

About 50 ml of *S. potatorum* seed powder extract was treated with 2 g of 0.1 M zinc nitrate to synthesize the ZnO NPs. These solutions were then agitated and treated with 1.0 M NaOH (10 ml) for 90 min at 60 °C. Then, the ions that initiated the reaction were generated by zinc nitrate in deionized water. The reaction mixture was incubated with constant stirring in the dark at 60 °C to avoid photocatalysis. After 24 h, the ZnO NPs were developed and were identified by half-white colour (Taha *et al.* 2020).

2.6. AC preparation

The methodology involved in this study included several steps for the preparation of AC from coconut shells. Initially, a metal pot was filled with small pieces of coconut shells, which were carbonized by cooking them on an open fire for 3–5 h. The resulting charcoal was then cleaned with water to remove impurities, followed by crushing it into smaller pieces using a mortar and pestle. The charcoal powder was air-dried for 24 h to eliminate any remaining moisture. Next, an activating agent was prepared by mixing calcium chloride and water in a 1:3 ratio, and the charcoal powder was immersed in this solution and allowed to soak overnight. Subsequently, the charcoal and activating agent mixture was heated at 300 °C for 3 h, resulting in the conversion of charcoal into AC. The AC was then cooled, transferred to a suitable storage container, and protected from moisture. This methodology provides a systematic approach for the preparation of AC from coconut shells, which can be utilized for water and air purification applications (Patel & Modi 2021).

2.7. Loading ZnO NPs on AC

After coating AC granules with ZnO NPs, to ensure that the coating was complete, 250 ml of the ZnO NP solution containing 0.1 M zinc nitrate was impregnated with 50 g of the treated AC granules while vigorously stirring at room temperature. The AC coated with ZnO was then cured in an incubator at 65–95 °C for at least 3 h. Measurements of the weight difference between the AC granules before and after coating the residual zinc in the solution following coating were used to confirm the preparation (Ivankovic *et al.* 2019).

2.8. Column filter design system

The column adsorption filter design consisted of a cylindrical column packed with a mixture of ZnO NPs and AC. The NPs were synthesized from *S. potatorum* seed extract using a green synthesis approach. AC is derived from a suitable precursor material. A cylindrical glass jar of volume 5 L with a bottom outlet was employed as a column to facilitate the removal of undissolved particles and contaminants while allowing the solvent to pass through. AC, derived from a suitable precursor material, underwent processing and impregnation with synthesized ZnO NPs. The filter bed was prepared by uniformly packing ZnO-impregnated AC particles in the column. The column had an internal diameter of 4 cm and a usable height of 15 cm. The ZnO-impregnated AC was filled to a height of 4 cm, followed by a layer of 4 cm of granular activated carbon (GAC) at the bottom and 2 cm of sterile cotton below the GAC layer, resting on a 1-cm gauze. The filter materials were packed in a specific order based on their pore size, as illustrated in Figure 1, with both layers tightly packed. A space of 5 cm at the top of the column was left to accommodate water. The time taken for water to traverse the column was measured at a flow rate of 50 ml/min.

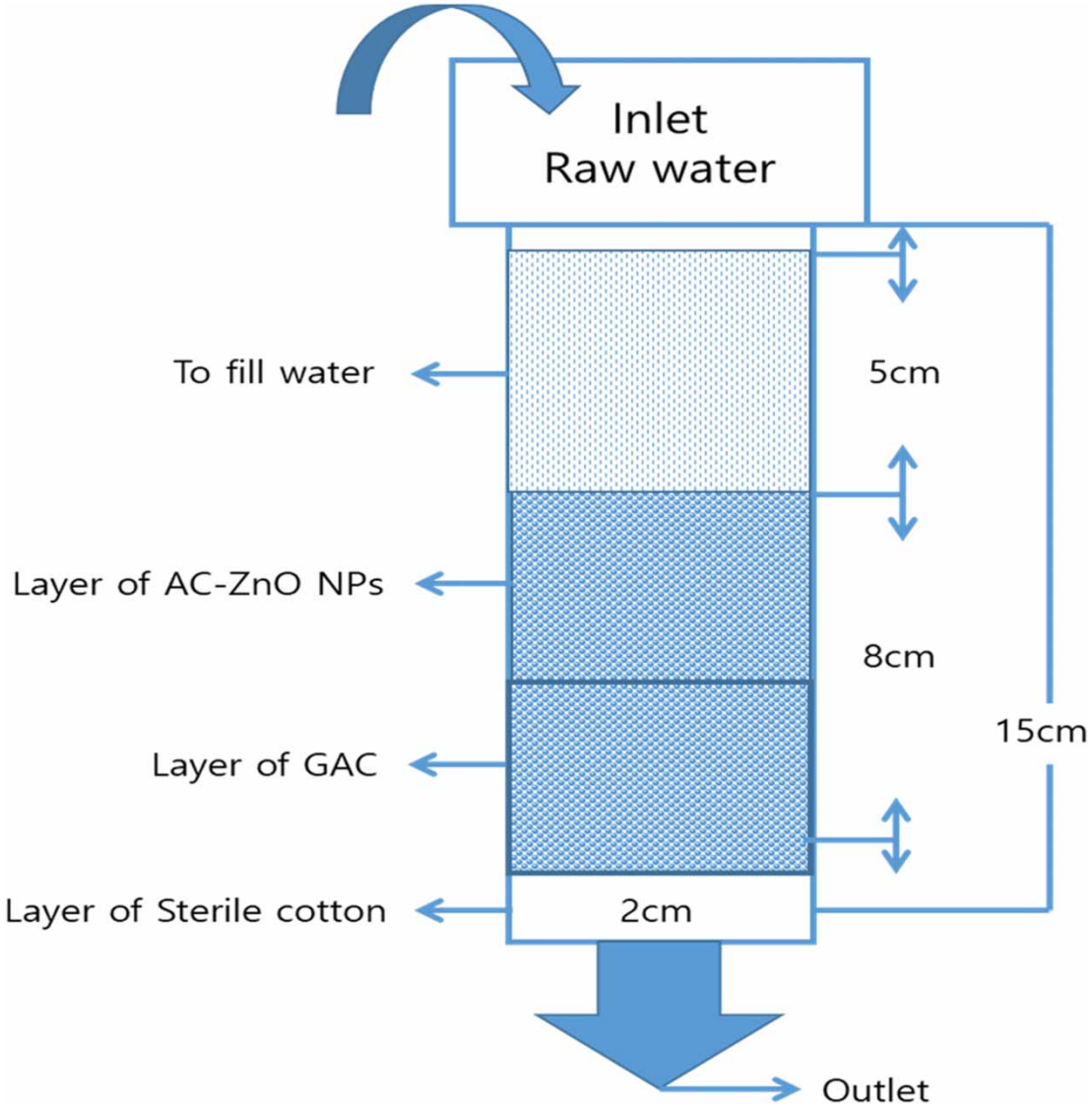

Figure 1 | Nanoadsorbent (ZnO NPs–AC) filter design.

2.9. Analysis of ZnO NPs (Taha *et al.* 2020)

ZnO NPs were analyzed in a Sophisticated Analytical Instrumentation Facility Centre, IIT (SAIF-IIT), Madras. The absorption spectra of NPs synthesized at different temperatures and concentrations allowed researchers to evaluate the optical properties of the ZnO NPs. A UV–visible spectrometer (Cary Series, Agilent Technologies) with a wavelength between 200 and 800 nm was used to characterize the samples. The spectral characteristics of the adsorbent were analyzed by scanning electron microscopy (SEM), XRD, and EDX analysis. The adsorbent was subjected to SEM to analyze its surface morphology. The crystalline structure of the ZnO NPs was studied using a Philips model PW 3710 XRD. On a JOEL JSM5900LV fitted with an EDX probe, SEM measurements were taken. A small layer of ZnO was applied to the loaded AC sample for SEM analysis.

2.10. Treatment of raw water with ZnO-AC NPs

Water treatment was carried out using the column adsorption filter system method. The synthesized ZnO NPs and water were added to 5-l glass jar. The pre-prepared ZnO-AC NPs were added to the column adsorbent filter at a dosage rate of 50 g, and the water dosage was approximately 1,000 ml in a 5-l glass jar. Designing fixed-bed nanoadsorbent systems on a large scale requires column studies, which demonstrate the economic

value of utilizing adsorbents. Undissolved and impurity particles could be eliminated as the solvent ran over a 5-l cylindrical glass jar with a bottom exit. A glass cylinder was filled with a column of ZnO NPs coated on AC. The column's interior diameter was 4 cm, and its usable height was 8 cm. The ZnO NPs with an AC coating was packed over 2-cm sterile cotton and 8 cm of ZnO-AC NPs layered over gauze in a column layer of width 1 cm, as depicted in Figure 1 and filter materials are packed in order of pore size. After packing both layers airtight, a 5-cm space was left at the top of the column. A flow rate of 45 ml/min was used to compute the amount of time required for water to run through the column (Azis *et al.* 2021).

The percentage of defluoridation was evaluated by the following Equation (1):

$$X = \frac{C_0 - C}{C_0} \times 100 \tag{1}$$

C_0 indicates the initial concentration of fluoride, C indicates the final concentration of fluoride, $X = (C_0 - C)$ indicates the amount of fluoride adsorbed.

2.11. Analysis of physiochemical parameters

The physicochemical compositions of the water samples were analyzed quantitatively and qualitatively as per the protocol of Trivedy & Goel (1986), and comparisons were made with the standard procedure used by American Public Health Association (APHA 2000). Water quality assessment involves the evaluation of physical and chemical parameters to determine their suitability for various purposes. The physical characteristics considered included appearance, colour, turbidity, odour, total dissolved solids (TDS), and electrical conductivity (EC). Chemical parameters such as pH, total solids (TS), total suspended solids (TSS), total hardness, calcium hardness, magnesium hardness, nitrates, nitrites, phosphates, sulphates, chlorides, fluorides, manganese, and total iron were also analyzed. These parameters were measured at the Tamil Nadu Water Analyzing Department (TWAD) laboratory in Krishnagiri.

2.12. Estimation of fluoride (Standard Method APHA 22nd edn, 2012)

A portion of the sample was diluted to 100 ml in a Nessler tube (V1). Zirconyl alizarin reagent (5 ml) was added, and the mixture was carefully blended and left for an hour in the dark. The amount of regular fluoride utilized in the comparison should be noted (V2). Double-distilled water was used to create standards from 0, 2, 4, 6, 8, 10, 12, and 14 ml (1 ml = 0.01 mg) to 100 ml. Then, 5 ml of zirconyl alizarin reagent was added, and the mixture was carefully blended and allowed to stand in the dark for 1 h. The standards used for comparisons were treated the same as those used for the sample.

Calculation:

$$'F'\ mg/l = \frac{100 \times \text{Standard (ml), which was compared} \times 10}{\text{Volume of sample}}$$

$$\text{Fluoride (mg/l)} = \frac{100 \times V_2 \times 10}{V_1}$$

2.13. Experimental analysis of adsorbent dosage

An adsorbent dosage of 10–50 g/1,000 ml of ZnO-AC NPs was used in the laboratory for the adsorption experiment. The adsorbent dosage was investigated separately using a continuous contact period of 2 h. After the sample was incubated for 2 h with ZnO-AC NPs, flocculation, impurities, and turbidity were removed by filtration. Following filtration, the percentage of the defluoridation equation is used to quantify the initial to maximum removal of an adsorbent capacity (Padmavathy *et al.* 2016).

$$E\% = \frac{C_0 - C}{C_0} \times 100$$

Adsorption efficiency ($E\%$) (2)

2.14. Statistical analysis

The data were analyzed using MS-Excel Autosum (∑), and the results are expressed as the mean ± standard deviation (SD). Each experiment was performed in triplicate. MS-Excel was used to plot the scatter plot and bar diagram graphs.

3. RESULTS AND DISCUSSION

3.1. Characterization of the adsorbent

3.1.1. UV–visible spectroscopy

UV–visible spectroscopy is typically used to confirm the synthesis of ZnO NPs. Electrons within a specific wavelength range start oscillating due to surface plasmon resonance (SPR). The UV–visible profile of the ZnO NPs was studied at wavelengths between 200 and 800 nm. The reaction mixture of zinc nitrate solution and aqueous seed extract from *S. potatorum* showed a peak in the UV–visible spectrum at 318 nm. This result suggested the presence of ZnO NPs as shown in Figure 2.

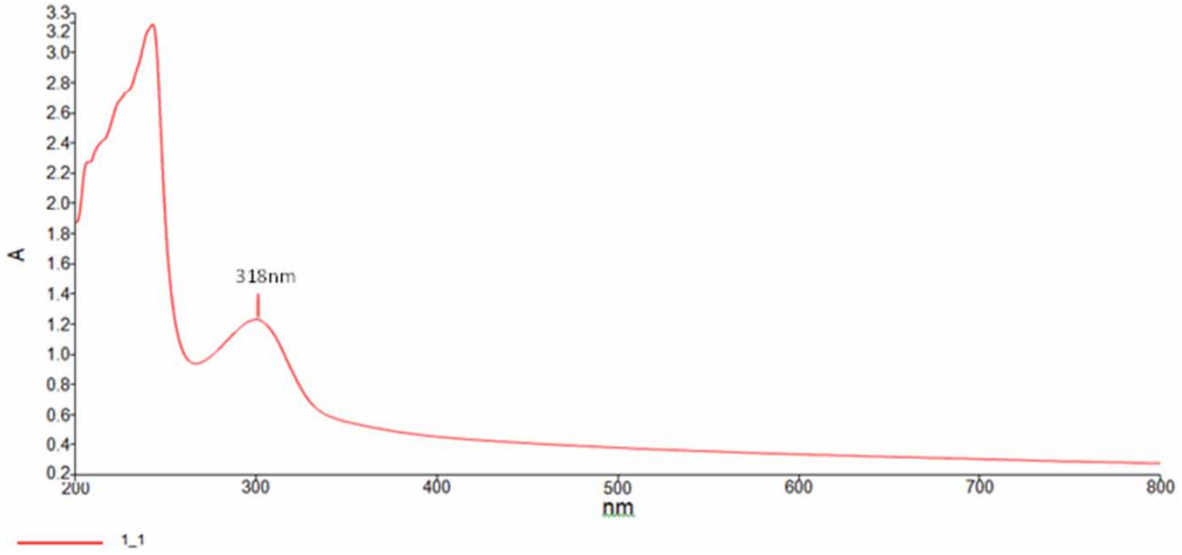

Figure 2 | UV–visible spectrum of synthesized ZnO-AC NPs.

Secondary metabolites present in plants facilitate the conversion of zinc ions from the surrounding solution into ZnO, with the plant extract serving as a stabilizing and reducing agent. This phenomenon was confirmed through the examination of UV–visible spectra spanning the wavelength range of 280–800 nm. Analysis of the spectra revealed a distinct peak at 320 nm, which is characteristic of ZnO NPs (Sasani Ghamsari *et al.* 2016). Additional findings by Ashwini *et al.* (2021) indicate that the absorbance peaks of ZnO NPs typically fall within the wavelength range of 310–360 nm.

3.1.2. HRSEM analysis

HRSEM was used to determine the size and morphology of the synthesized ZnO NPs. As depicted in Figure 3(a) and 3(b), the ZnO particles were spherical and of different sizes and highly agglomerated. The SEM image shows the high density of ZnO NPs synthesized from *S. potatorum* seed extract. SEM analyses confirmed the face-centred cubic structure of the NPs. The sizes of the spherical and hexagonal particles ranged from 260 to 330 nm, respectively. The overlaying of particles on top of each other caused the size to increase.

The size and shape of the synthesized NPs were examined using SEM images captured at various magnifications. The surface morphology confirmed the formation of NPs in their agglomerated form. Several studies have evaluated the relationship between surface shape and the synergistic action of ZnO (Datta *et al.* 2017). The majority of the particles were determined to be horizontal, and XRD further supported this conclusion.

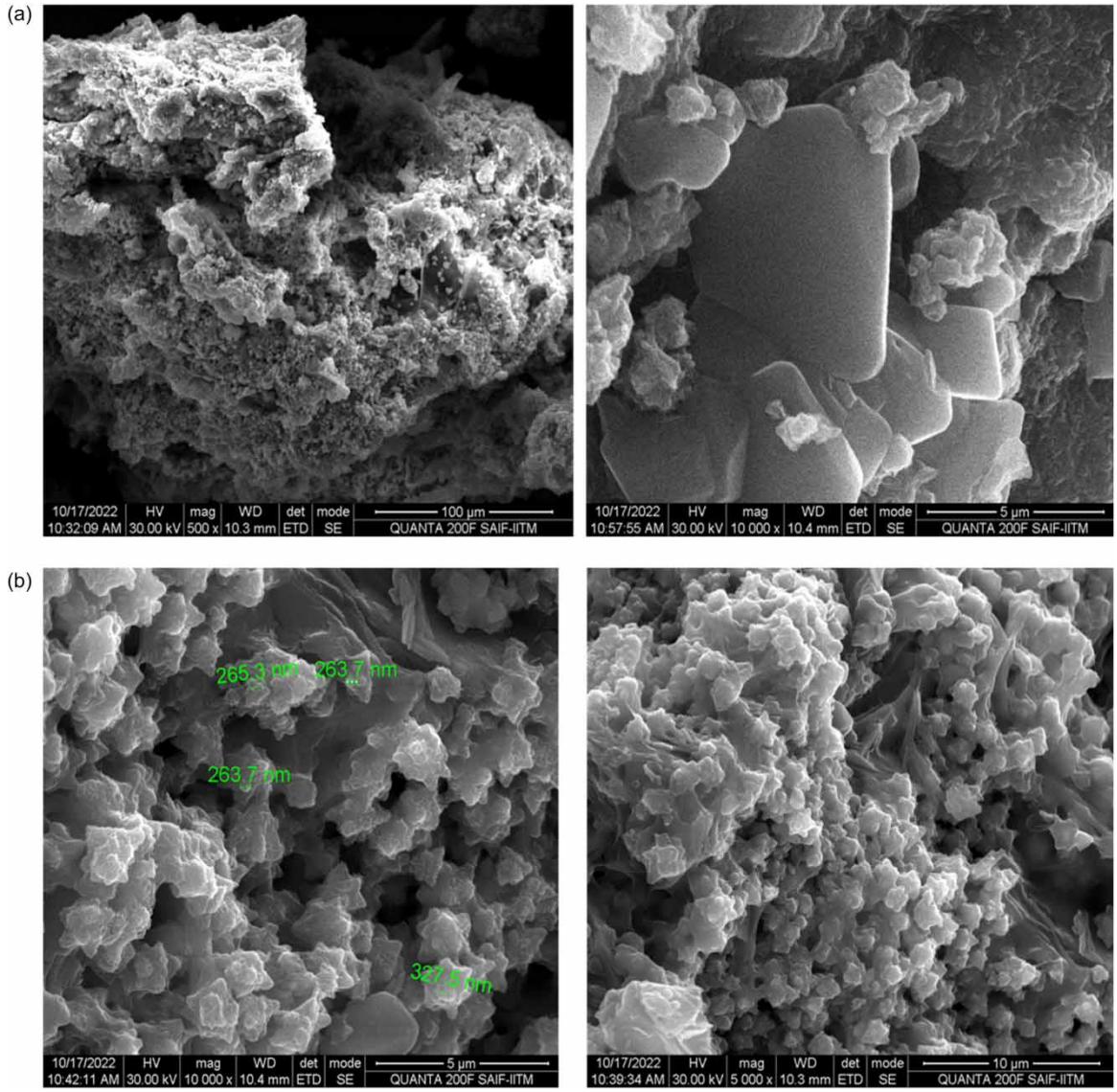

Figure 3 | High-resolution scanning electron microscopy (HRSEM).

3.1.3. Energy-dispersive spectroscopy analysis of the ZnO NPs

The elemental composition of the reaction mixture was determined using energy-dispersive spectroscopy (EDS), as shown in Figure 4(a) and 4(b). The analysis of the EDS spectra confirmed the formation of ZnO NPs. The atomic weight of oxygen accounted for 50.27% of the total weight, with a weight percentage of 33.24%. Similarly, the atomic weight of zinc represented 19.09% of the total weight, with a weight percentage of 51.55%.

Furthermore, EDS analysis of the NPs revealed the presence of ZnO NPs. Oxygen accounted for 68.39% of the total atomic weight (34.62%), while zinc accounted for 31.61% of the total atomic weight (65.38%). These findings demonstrated the significant presence of the zinc (Zn) phase in the synthesized ZnO NPs.

The EDS peaks indicated a prominent peak at 78.32% for zinc and 12.78% for oxygen, closely resembling the reported weight percentages for the fabrication of ZnO NPs. This information provides valuable insights into the elemental composition of the analyzed NPs. Specifically, zinc exhibited distinct peaks at 1 and 8.6 eV, while oxygen displayed a signal at 0.5 eV, aligning with the characteristic energy values for zinc and oxygen, respectively. These observations further confirm the elemental makeup of the synthesized compound as ZnO. Additionally, EDS analysis detected traces of other substances, such as sodium, along with zinc and oxygen in the NPs, as previously reported (Fakhari & Jamzad 2019; Ashwini *et al.* 2021).

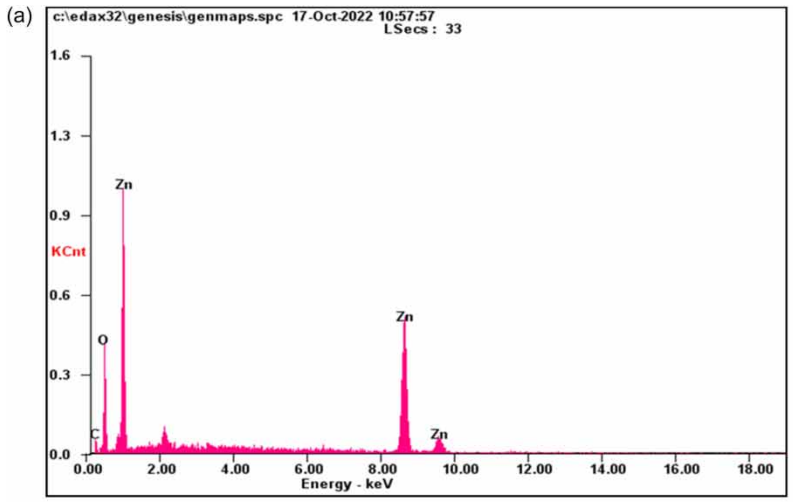

Element	Wt%	At%
CK	15.21	30.64
OK	33.24	50.27
ZnK	51.55	19.09
Total	100%	

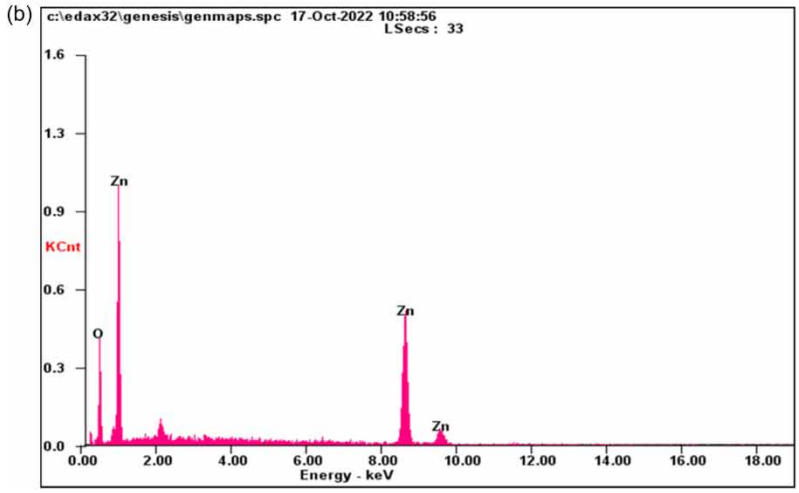

Element	Wt%	At%
OK	34.62	68.39
ZnK	65.38	31.61
Total	100%	

Figure 4 | Elemental composition of synthesized ZnO-AC NPs.

3.1.4. XRD spectroscopy

XRD analysis was also conducted on the ZnO NPs to determine their crystallinity. The XRD pattern, shown in Figure 5, revealed the presence of distinct peaks corresponding to the crystal structure and crystallite size of the particles. According to the Joint Committee on Powder Diffraction Standards (JCPDS), the observed XRD peaks at 2θ values of 31.8°, 34.5°, 36.2°, 47.5°, 56.6°, 62.8°, 66.4°, 67.9°, 69.1°, and 77.1° corresponded to the (100), (002), (101), (102), (110), (103), (200), (112), (201), and (202) crystallographic planes, respectively, of a hexagonal crystal geometry. To determine the average particle size of the ZnO NPs, the Scherrer equation was used.

$$D = \frac{K\lambda}{\beta \cos \theta} \tag{3}$$

This equation utilizes the Scherrer constant ($K = 0.9$), the wavelength of the incident light used for diffraction ($\lambda = 1.54$ Å), the full width at half maximum (FWHM) of the diffraction peak (β), and the reflection angle (θ). The calculated average size of the ZnO NPs was found to be 48 nm.

The XRD analysis confirmed the crystalline nature of the ZnO NPs. The diffractogram displayed the intensity of the diffracted rays as a function of the diffraction angle. Furthermore, the shape of the NPs was determined to be hexagonal, consistent with previously reported values of lattice parameters a (=b) = 3.2568 Å and c = 5.2125 Å (Fardood *et al.* 2017). Additionally, the XRD results provided evidence for the successful synthesis of

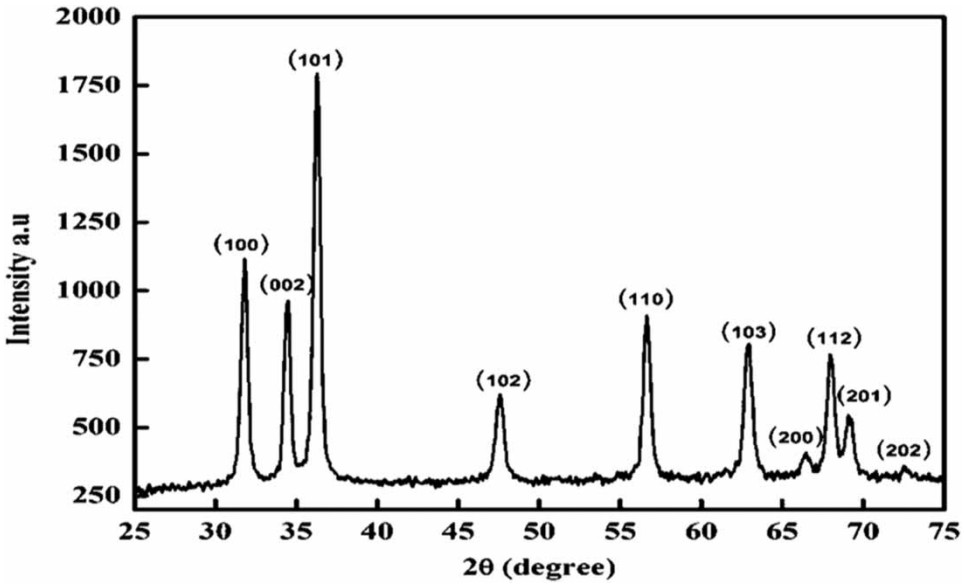

Figure 5 | XRD patterns of synthesized ZnO-AC NPs.

the nanoadsorbent, revealing characteristic peaks corresponding to both ZnO NPs and AC. SEM images demonstrated a uniform distribution of NPs on the surface of the AC, indicating effective impregnation.

3.2. Physiochemical analysis of the raw water

According to the findings presented in Table 1, the deep soil water samples collected from the Dharmapuri district exhibited significant variations in various physicochemical characteristics. These measurements were compared to the Indian and WHO standards. Analysis of the raw water sample revealed a wide range of calcium (Ca^{2+}) ion concentrations, with values ranging from 132 mg/l. Similarly, the concentration of magnesium (Mg^{2+}) ions ranged between 83 mg/l. The pH of the sample was recorded as 7.95, while the TDS concentration was 1,850 mg/l. Notably, the chloride content was found to be 423 mg/l, surpassing the permissible limit. Taken together, the obtained results suggest that the water quality in this region is unsuitable for human consumption, as indicated by the parameters falling outside the acceptable range.

Maskey *et al.* (2020) reported that high TDS levels in water are neither toxic nor harmful. However, they may affect people with heart or kidney disorders or cause constipation in healthy individuals, resulting in the use of laxatives. According to the findings of Thirupathi & Muniyan (2018), the examination of water samples obtained from various villages in the Dharmapuri district demonstrated that the water quality parameters, including pH, EC, total alkalinity, total hardness, calcium hardness, magnesium hardness, chloride, nitrate, fluoride, and TDS, exceeded the permissible limits set by the BIS, Indian Council of Medical Research (ICMR) and WHO standards. The outcomes of the present investigation suggest that the drinking water consumed by residents in the villages of Dharmapuri district is not suitable for consumption. Taken together, the present study results highlight significant concern regarding the chosen geographical region. The villages of Dharmapuri District are mostly affected by water contamination, and all the parameters were found to exceed permissible limits, which can render the water unpalatable and potentially harmful if consumed in consistently large quantities.

3.3. Permissible limits of physiochemical parameters in drinking water

The WHO and the ICMR have established permissible limits for physiochemical parameters to ensure the quality of drinking water. Table 1 provides the maximum allowable levels of physiochemical parameters in deep soil water.

3.4. Measurement of fluoride levels in raw water

Fluoride, a mineralized form of the halogen element fluorine with the chemical symbol F, is necessary for healthy human growth, development, and maintenance. Flourine occurs naturally in food, water, air, and soil. Excess fluoride exposure can affect thyroid issues, bone tissues, skeletal fluorosis and brain stimuli. Fluoride levels in water

Table 1 | The physiochemical analysis of raw water and nanoadsorbent-treated water samples in Dharmapuri zones compared with standard values

		Dharmapuri zone		
S. No	**Experiments**	**Raw water**	**Nanotreated**	**Standard permissible limit**
Physical examinations				
1	Appearance	Clear	Clear	Clear
2	Colour (pt.co-scale)	Colourless	Colourless	5
3	Odour	None	None	Unobjectable
4	Turbidity NTU	2.8 ± 0.02	2.0 ± 0.12	5
5	Total dissolved solids mg/l	1,850 ± 13	795 ± 9.4	500
6	Electrical conductivity mic mho/cm	2,351 ± 8.6	876 ± 3.5	–
Chemical examinations units mg/l				
7	pH	8.1 ± 0.2	7.43 ± 0.23	7.0–8.5
8	Alkalinity total as $CaCo_3$	570 ± 2.05	548 ± 3.5	200
9	Total hardness as $CaCo_3$	664 ± 0.81	592 ± 1.6	300
10	Calcium as Ca	132 ± 1.06	65 ± 0.43	75
11	Magnesium as Mg	83 ± 1.2	45 ± 0.75	50
12	Iron total as Fe	0	0.13	0.3
13	Manganese as Mn	0	0	0.1
14	Free ammonia as NH_3	0	0.09	0.5
15	Nitrite as NO_2	0.01	0	–
16	Nitrate as NO_3	41 ± 0.76	23 ± 1.1	20
17	Chloride as Cl	423 ± 1.24	165 ± 0.23	250
18	Sulphate as SO_4	135 ± 0.81	124 ± 1.4	200
19	Phosphate as PO_4	0.02	0	–

Note: Values are expressed as average concentration of mean ± SD. All units except pH are in mg/l, otherwise stated.

were measured using the KIT method. Table 1 shows the analysis of the physiochemical status of the raw water samples collected from Dharmapuri. The fluoride concentration was calculated using the drop titration method and an Aquasol test kit (AE210, Rakiro Biotech). The fluoride concentration in the raw water sample was 6.0 mg/l (Table 2). The results showed that the fluoride concentration in the water sample was very high and exceeded three-fold greater than the potable limit. This finding confirmed that the Dharmapuri district water was highly contaminated with fluoride and the water quality was not good enough to drink.

Table 2 | The fluoride status of raw water and nanoadsorbent-treated water sample in Dharmapuri zones

		Dharmapuri zone			
S. No	**Experiments**	**Raw water**	**Nano treated**	**WHO Permissible limit**	**ICMR Permissible limit**
1	Fluoride as F^-	6 ± 0.45	1.2 ± 0.12	1.0	1.5

Note: Values are expressed as average concentration of Mean ± SD in fluoride ranges in raw, nano treated water samples and compared with drinking water Standards of ICMR and WHO. Fluoride expressed as F^- in mg/l otherwise stated.

In the research study conducted by Thirupathi & Muniyan (2018), an analysis of water samples from various villages in Dharmapuri district demonstrated that the fluoride levels in the water exceeded the permissible limits set by the BIS, ICMR, and WHO standards. Among all the parameters examined, there was a significant issue regarding excessively high concentrations of fluoride, nitrate, chloride, and TDS. Merely 55% of the water samples exhibited fluoride contents within the permissible limit (>1.5 mg/l, WHO), while the remaining 46% of villages displayed considerably elevated fluoride concentrations. This increase in fluoride in water can be attributed to the presence of a fluoride-rich rock salt system. Excessive

fluoride intake can potentially lead to tooth decay, kidney disease and many neurological disorders. However, the findings of our study suggest that the water consumed by the inhabitants of villages in Dharmapuri district is not suitable for consumption.

3.5. Water treatment using nanoadsorbents (ZnO-impregnated AC)

3.5.1. Experimental setup

The effectiveness of a nanoadsorbent filtering system was tested using a glass jar column adsorbent at various concentrations. The nano-metal adsorbent was utilized to eliminate turbidity and natural organic detritus. In comparison to other methods, this approach offers several advantages, including the absence of chemicals, low cost, simple use while maintaining effectiveness, and safe human health. Filtration methods, such as dissolved particles, bacteria, viruses, parasites, dust, and chemicals, are commonly employed to separate solid matter (flocs) from fluid. The filter consisted of multiple layers, including ZnO NPs-AC, sterile cotton, and micropore-sized layers. These layers were designed to purify the water and ensure efficient treatment. Sterile cotton was added to prolong the retention period, while the final layer of ZnO-AC facilitated the removal of water impurities and unpleasant odours.

3.5.2. Water analysis calculations

To assess the efficiency of the nanoadsorption, water samples were analyzed before and after the addition of the ZnO-AC nanoadsorbent.

$$E\% = \frac{C_0 - C}{C_0} \times 100 \tag{4}$$

Adsorption efficiency ($E\%$)

The ancient practice of using *S. potatorum* seeds to clarify water quality, dating back to 4000 BC, demonstrates the long-standing interest in water purification (Vijay & Waman 2017). This species, commonly known as Nirmali or the clearing nut tree, is a medium-sized tree primarily utilized for its medicinal properties. It can be found in southern and central India, Sri Lanka, and Burma. In this study, ZnOZnO NPs were synthesized using *S. potatorum* seed powder. ZnO is an important component for various industrial applications, and its effectiveness against different microbial strains has been well documented. ZnO NPs have the potential to enhance water and wastewater treatment processes by improving their efficacy. These NPs are considered promising materials for water purification due to their desirable physiochemical properties (Spoiala *et al.* 2021).

3.6. Physiochemical levels in nanoadsorbent-treated water

A pH of 7.43 was observed in the treated water, and the TDS concentration was 795 mg/l. There was no discernible change in the pH. The concentration of calcium ions was 65 mg/l, while the concentration of magnesium ions was 45 mg/l. The chloride content was 165 mg/l, and the total iron, nitrite, nitrate, sulphate and phosphate concentrations were within permissible limits. Table 1 shows the considerable reduction in the hardness of water with ZnO NP–AC. In addition, the success of nanofiltration was attributed to the enhanced taste of the treated water. Nanofiltration has successfully removed turbidity, odour, hardness and toxicity from water, improving the potability of the water. The water samples that were obtained from outside the column were fit for human health and nutritional needs for irrigation.

Most physicochemical parameters of treated water are within acceptable ranges, improving water quality and meeting human and agricultural nutritional needs. Using treated water for irrigation might be a good solution to the problems of untreated contaminated water and water scarcity (Hashem and Qi 2021). According to Chauque *et al.* (2016), in this study, ZnO ENPs were effectively eliminated from wastewater, with only a negligible amount of ZnO ENPs discharged into the environment through the treated effluent. Since the 1950s, research on the antibacterial properties of ZnO has been conducted. Like other oxides such as calcium and magnesium, ZnO exhibits microbicidal activity against bacterial strains (Wang *et al.* 2017). Therefore, our results suggest that the impregnation of AC with ZnO NPs is a promising physiochemical approach for efficient water treatment.

3.7. Defluoridation assessment utilizing a composite of nanoadsorbent ZnO-AC NPs

3.7.1. Measurement of fluoride levels in nanoadsorbent-treated water

Fluoride-contaminated water samples were collected from the pappireddipatti region in the Dharmapuri district, after which water was added to the column for adsorption. The experimental results demonstrated the efficacy of the nanoadsorbent for removing fluoride. The initial fluoride concentration ranged between 5.3 and 6.0 mg/l. After passing through the column packed with the nanoadsorbent, the final fluoride concentration decreased significantly. The results for the treated water are shown in Table 2. In Dharmapuri district, the average concentration was 1.2 ± 0.08 mg/l. The results indicated that the ZnO NPs impregnated with AC exhibited superior fluoride removal efficiency.

Norhusna *et al.* (2019) conducted a study wherein they successfully demonstrated the synthesis of modified graphene oxide (GO) with ZnO as an adsorbent for the purpose of fluoride removal. Through their experimental investigations, they explored several synthesis parameters and observed that the modified GO/ZnO NPs exhibited promising potential as an effective adsorbent for fluoride removal in wastewater. Moreover, the present study revealed the high efficiency of the nanoadsorbent in removing fluoride from water. The final fluoride concentrations were significantly lower than the initial concentrations, indicating successful adsorption. The efficiency of fluoride removal increased with increasing adsorbent dosage and longer contact time.

3.7.2. Percentage of defluoridation using nanoadsorbent composite

The percentage of defluoridation was evaluated using the following equation:

$$X = \frac{C_0 - C}{C_0} \times 100$$

C_0 is the initial concentration of fluoride, C is the final concentration of fluoride, and X is the amount of fluoride adsorbed (C_0–C).

At an initial concentration of 6.0 mg/l, the nanoadsorbent demonstrated an average defluoridation efficiency of 65% after a 30-minute contact time. A comparison of these findings and Table 3, where the concentration of fluoride in the raw water samples containing 6.0 mg/l was effectively reduced by 80%, it is evident that treatment with the nanoadsorbent (ZnO-AC) packed in an adsorbent column efficiently removed colour, white fluoride, floc, coagulant, and turbidity through the adsorbent composite material. The above results suggest that the adsorbent possesses significant potential for reducing the fluoride concentration in water samples, with the degree of defluoridation dependent on the initial fluoride concentration and contact time.

Table 3 | The percentage of defluoridation efficiency

		Dharmapuri zone		
S. No	Experiments	Raw water initial F^- Conc. mg/l	Nano adsorbent Final F^- Conc. mg/l	Efficiency in % $\% = \frac{C_0 - C}{C_0} \times 100$
1	Fluoride as F^-	6	1.2	80%

Note: Values are expressed as fluoride ranges in raw water samples and nano adsorbent water samples its shows the F^- removal efficiency in %. Fluoride expressed as F^- in mg/l otherwise stated.

ZnO NPs serve as highly efficient catalysts due to their relatively large surface area and the pronounced effects of their small quantum size. The enhanced adsorption efficiency of the NPs can be attributed to their increased adsorption capacity as adsorbents, facilitated by their high surface area and greater density of adsorption sites (Bazrafshan *et al.* 2016). In line with the findings of Mahvi *et al.*'s study (2020), the adsorption efficiency improved with increasing contact time. However, an increase in the amount of the ZnO NP adsorbent resulted in decreased removal efficiency. Based on our present study results, it can be concluded that the adsorption of fluoride by ZnO NPs represents an efficient and reliable method for removing F from water solvents.

3.7.3. Effect of adsorbent dosage on fluoride removal

The effect of adsorbent dosage is presented in Figure 6. The outcome is that an increase in the adsorbent weight from 10 to 50 g/1,000 ml decreases the fluoride clearance percentage. At doses of 10 g/1,000 ml, 20 g/1,000 ml,

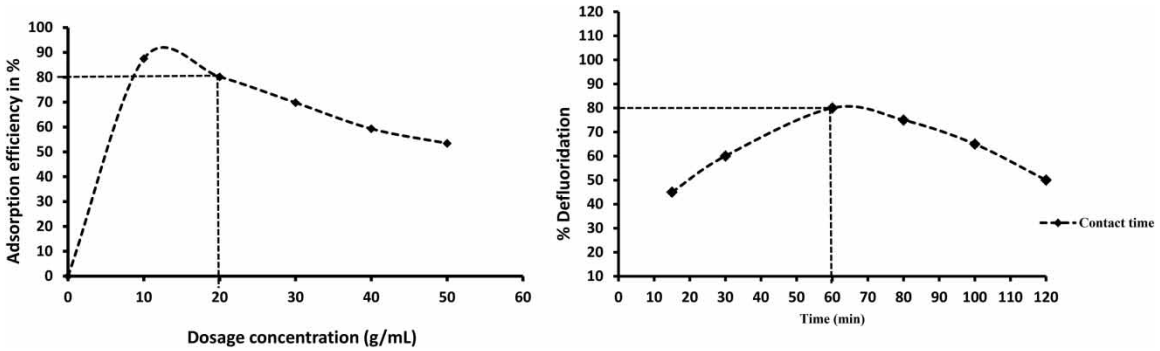

Figure 6 | Adsorption efficiency against ZnO-AC NP dose.

30 g/1,000 ml, 40 g/1,000 ml, and 50 g/1,000 ml, the percentages of defluoridation after ZnO-AC NP treatment were 87.5, 80.5, 69.8, 59.3, and 53.4%, respectively, after the maximum contact period of 2 h. These results confirmed that the ZnO NPs impregnated with AC exhibited excellent defluoridation efficiency. At an optimum adsorbent dosage of 20 g/l, the fluoride removal efficiency reached 80.5% for a contact time of 60 min. The results indicate that the adsorbent performance improves with longer contact time, allowing more fluoride ions to be adsorbed onto the surface of the NPs.

In his study, Mahvi *et al.* (2020) observed ZnO NPs to be efficient adsorbents for removing fluoride (F) from aqueous solutions with ZnO NPs. F can be removed from aqueous solution by adjusting the pH, contact time, and adsorbent dosage. A longer contact time more effectively promoted adsorption. Additionally, the removal efficiency decreased as the amount of the ZnO NP adsorbent increased. The maximum F removal was attained after 60 min at pH 6 and 0.02 g/l adsorbent, with an initial F concentration of 20 mg/l. The effectiveness of this material was 97.5% at an ideal pH of 6 and a 0.06 g/l adsorbent dose with 60 min of contact time for a 20 mg/l initial fluoride concentration. However, in our present study, within a contact time of 60 min, the defluoridation efficiency increased to 80%. The findings of this study suggest that the nanoadsorbent ZnO NPs impregnated with AC can be a reliable option for defluoridation of water in the Dharmapuri district. The adsorbent demonstrated substantial defluoridation efficiency and its performance could be further enhanced by optimizing the contact time between the adsorbent and water samples.

4. CONCLUSION

The key phase of our present study in nanotechnology is the development of eco-friendly green-synthesized ZnO NPs using *S. potatorum* seed extract, a natural resource. The bio-natural resource, NPs are not only safe and eco-friendly but found effective in filtration process. This investigation confirmed that the composite material impregnating ZnO NPs into an activated carbon (ZnO-AC NPs) column has exhibited excellent adsorption potency. UV–visible spectral analysis, XRD, HRSEM, and EDX confirmed the successful synthesis of ZnO-AC NPs from *S. potatorum* seed extract, and EDX spectroscopy provided valuable insights into the elemental composition. These analytical reports confirm the successful synthesis of the ZnO-AC NPs. The effectiveness of the coating on AC was confirmed by the fluoride concentration in the filtrate solution. The AC acted as a basal column matrix, providing a large surface area for the ZnO-AC NPs to bind and resorb fluoride ions from the water. Success of our goal was numerical percentage of the defluoridation rate effective to that of AC column. Future study is to evaluate antioxidant potential of filtrate obtained from eco-friendly green-synthesized column.

AUTHOR CONTRIBUTIONS

All the authors reviewed the study conception and design; collected data and did analyses; and interpreted results and approved the final version of the manuscript.

FUNDING INFORMATION

There was no funding agency support; it was only a self-supported project.

DATA AVAILABILITY STATEMENT

Data cannot be made publicly available; readers should contact the corresponding author for details.

CONFLICT OF INTEREST

The authors declare there is no conflict.

REFERENCES

Ahmad, S., Singh, R., Arfin, T. & Neeti, K. 2022 Fluoride contamination, consequences and removal techniques in water: A review. *Environmental Science Advances* **1**, 620–661. https://doi.org/10.1039/d1va00039j.

Al-Hazmi, H. E., Luczak, J., Habibzadeh, S., Hasanin, M. S., Mohammadi, A., Esmaeili, A., Kim, S. J., Khodadadi Yazdi, M., Rabiee, N., Badawi, M. & Saeb, M. R. 2024 Polysaccharide nanocomposites in wastewater treatment: A review. *Chemosphere* **347**, 140578. https://doi.org/10.1016/j.chemosphere.2023.140578.Epub.

APHA. 2000 *American Public Health Association and Water Pollution Control Federation*, 15th edn.. Washington, DC, pp. 12–56.

APHA, AWWA, WEF 2012 *Standard Methods for Examination of Water and Wastewater*, 22nd edn. American public health association, Washington, DC.

Ashwini, J., Aswathy, T. R. & Achuthsankar, S. N. 2021 Green synthesis and characterization of nanoparticles using Cayrata Pedata leaf extract. *Biochemistry and Biophysics Reports* **26**, 100995, https://doi.org/10.1016/j.bbrep.2021.100995.

Azis, K., Mavriou, Z., Karpouzas, D. G., Ntougias, S. & Melidis, P. 2021 Evaluation of sand filtration and activated carbon adsorption for the post – treatment of a secondary biologically – treated fungicide containing wastewater from fruit–packing industries. *Processes* **9**, 1223. https://doi.org/10.3390/pr9071223.

Bazrafshan, E., Balarak, D., Panahi, A. H., Kamani, H. & Mahvi, A. H. 2016 Fluoride removal from aqueous solutions by cupric oxide nanoparticles. *Fluoride* **49**(3), 233–244.

Chauque, E. F. C., Zvimba, J. N., Ngila, J. C. & Musce, N. 2016 Fate, behavior and implications of ZnO nanoparticles in a stimulated wastewater treatment plant. *Water SA* **42**(1). https://dx.doi.org/10.4314/wsa.v42il.09.

Datta, A., Patra, C., Bharadwaj, H., Kaur, S. & Dimri, N. 2017 Green Synthesis of Zinc Oxide Nanoparticles Using Parthenium hysterophorus Leaf Extract and Evaluation of their Antibacterial Properties. *J. Biotechnol Biomater* **7**, 271. https://doi.org/10.4172/2155-952X.1000271.

Elhalil, A., Qourzal, S., Mahjoubi, F. Z., Elmoubarki, R., Farnane, M., Tounsadi, H., Sadiq, M., Abdennouri, M. & Barka, N. 2016 Defluoridation of groundwater by calcined Mg/Al layered double hydroxide. *Emerging Contaminants* **2**(1), 42–48. https://doi.org/10.1016/j.emcon.2016.03.002.

Fakhari, S. & Jamzad, K. F. H. 2019 Green synthesis of Zinc oxide nanoparticles: A comparison. *Green Chemistry Letters and Reviews* **10**, 19–24. https://doi.org/10.10801/17518253.2018.1547925.

Fardood, S. T., Ramazani, A., Moradi, S. & Asiabi, P. A. 2017 Green synthesis of zinc oxide nanoparticles using Arabic gum and photocatalytic degradation of direct blue 129 dye under visible light. *Journal of Materials Science: Materials in Electronics* **28**, 13596–13601. https://doi.org/10.1007/s10854-017-7199-5.

Gao, M., Wang, W., Yang, H. & Ye, B. C. 2020 Efficient removal of fluoride from aqueous solutions using 3D flower-like hierarchical zinc-magnesium-aluminium ternary oxide microspheres. *Chemical Engineering Journal* **380**, 122459. https://doi.org/10.1016/j.ceramint.2016.09.181.

Hashem, M. S. & Qi, X. 2021 Treated wastewater irrigation – A review. *Water* **13**(11), 1527. https://doi.org/10.3390/w13111527.

Ivankovic, T., Dikic, J., du Roscoat, S. R., Dekic, S., Hrenovic, J. & Ganjto, M. 2019 Removal of emerging pathogenic bacteria using metal-exchanged natural zeolite bead filter. *Water Science and Technology* **80**(6), 1085–1098. https://doi.org/10.2166/wst.2019.348.

Joshi, S., Bajpai, S. & Jana, S. 2020 Application of ANN and RSM on fluoride removal using chemically activated D. sissoo sawdust. *Environmental Science and Pollution Research* **27**, 17717–17729. https://doi.org/10.1038/s41598-019-54902-8.

Joshua Amarnath, D., Nethaji Mariappan, E., Anne Beaula, M. & Vadivel, N. 2015 Evaluating fluoride contamination in groundwater of Dharmapuri district in Tamil Nadu. *Journal of Chemical and Pharmaceutical Sciences* **8**(1), 18–25.

Kashyap, S. J., Sankannavar, R. & Madhu, G. M. 2021 Fluoride sources, toxicity and fluorosis management techniques – A brief review. *Journal of Hazardous Materials Letters* **2**, 100033. https://doi.org/10.1016/j.hazl.2021.100033.

Kumar, S. 2023 Smart and innovative nanotechnology applications for water purification. *Hybrid Advances* 100044. https://doi.org/10.1016/j.hybadv.2023.100044.

Lu, W., Zhang, C., Du, Y., Quan, B., Qin, Z., Cheng, K., Niyazi, A. & Su, P. 2023 Applications of nanoadsorbents for the removal of fluoride from water: Recent advancements and future perspectives. *Separation & Purification Reviews*. https://doi.org/10.1080/15422119.2023.2280956.

Mahvi, A., Mostafapour, F. & Balarak, D. 2019 Adsorption of fluoride from aqueous solution by eucalyptus bark activated carbon: Thermodynamic analysis. *Fluoride* **52**(4), 562–568.

Mahvi, A. H., Rahdar, A., Igwegbe, C. A., Rahdar, S. & Ahmadi, S. 2020 Fluoride removal from aqueous solutions by zinc oxide nanoparticles. *Fluoride* **53**(3), 531–541.

Maity, J. P., Hsu, C. M., Lin, T. J., Lee, W. C., Bhattacharya, P. & Bundschuh, J. 2018 Removal of fluoride from water through bacterial-surfactin mediated novel hydroxyapatite nanoparticle and its efficiency assessment: Adsorption isotherm, adsorption kinetic and adsorption Thermodynamics. *Environ Nanotechnology, Monit Manag* **9**, 18–28. https://doi.org/10.1016/j.enmm.2017.11.001.

Maskey, M., Annavarapu, L. S., Prasai, T. & Bhatta, D. R. 2020 Physical, chemical and microbiological analysis of bottled water in Pokhara, Nepal. *Journal of Chitwan Medical College* **10**(2), 25–28. Available from: https://nepjol/index.php/JCMC/article/view/29664

Naga, D. K. R. C., Gomathi Nagajothi, P., Natrayan, L., Reddy, Y. B. S., Veeman, D., Patil, P. P. & Thanappan, S. 2022 Investigation on efficient removal of fluoride from groundwater using activated carbon adsorbents. *Adsorption Science & Technology* **7948069**, 9. https://doi.org/10.1155/2022/7948069.

Norhusna, M. N., Rodi, M. H. M. & Amri, N. 2019 Synthesis of GO-ZnO via impregnation method for fluoride removal in waste water. *ESTEEM Academic Journal* **15**, 35–48.

Padmavathy, K. S., Madhu, G. & Haseena, P. V. 2016 A study on effects of pH, adsorbent dosage, time, initial concentration and adsorption isotherm study for the removal of hexavalent chromium (Cr(VI)) from wastewater by magnetite nanoparticles. *Procedia Technology* **24**, 585–594. https://doi.org/10.1016/j.protcy.2016.05.127.

Patel, S. & Modi, P. 2021 Production of activated carbon from coconut shell. *International Journal of Creative Research Thoughts* **9**(11).

Prabu, K. M., Arivuselvam, L., Suguna, K., Subramani, K., Arulmoji, V. & Anbarasan, P. M. 2014 Synthesis of silver particles using the extracts of Strychnos potatorum. *NSNTAIJ* **8**(4), 130–137.

Rashid, U. S., Das, T. K., Sakthivel, T. S., Seal, S. & Bezbaruah, A. N. 2021 GO-CeO2 nanohybrid for ultra-rapid fluoride removal from drinking water. *Science of the Total Environment* **1**(793), 148547. https://doi.org/10.1016/j.scitotenv.2021.148547.

Rasool, A., Farooqi, A. & Xiao, T. 2018 A review of global outlook on fluoride contamination in groundwater with prominence on the Pakistan current situation. *Environmental Geochemistry and Health* **40**, 1265–1128. https://doi.org/10.1007/s10653-017-0054-z.

Ren, C., Li, H. H., Zhang, C. Y. & Song, X. C. 2022 Effects of chronic fluorosis on the brain. *Ecotoxicology and Environment Safety* **1**(244), 114021. https://doi.org/10.1016/j.ecoenv.2022.114021.

Sasani Ghamsari, M., Alamdari, S., Han, W. & Park, H. 2016 Impact of nanostructured thin ZnO film in ultraviolet protection. *International Journal of Nanomedicine* **12**, 207–216. https://doi.org/10.2147/IJN.S118637.

Saxena, K. L. & Sewak, R. 2015 Fluoride consumption in endemic villages of India and its remedial measures. *International Journal of Engineering Science Invention* **4**(1), 58–73.

Singh, J., Singh, P. & Singh, A. 2016 Fluoride ions vs removal technologies: A study. *Arabian Journal of Chemistry* **9**, 815–824. http://dx.doi.org/10.1016/j.arabjc.2014.06.005.

Sonal, S., Prakash, P., Mishra, B. K. & Nayak, G. C. 2020 Synthesis, characterization and sorption studies of a zirconium(iv) impregnated highly functionalized mesoporous activated carbons. *RSC Advances* **10**(23), 13783–13798. https://doi.org/10.1039/c9ra10103a.

Spoiala, A., Ilie, C., Trusca, R. D., Opera, O. C., Surdu, V. A., Vasile, B. S., Ficai, A., Ficai, D., Andronescu, E. & Ditu, L. M. 2021 Zinc oxide nanoparticles for water purification. *Materials (Basel)* **14**(16), 4747. https://doi.org/10.3390/ma14164747.

Taha, A., Aissa, M. B. & Da'na, E. 2020 Green synthesis of an activated carbon-supported Ag and ZnO nanocomposite for photocatalytic degradation and its antibacterial activities. *Molecules* **25**, 1586. https://doi.org/10.3390/molecules25071586.

Thirupathi, S. & Muniyan, M. 2018 Evaluating fluoride contamination in groundwater samples of Dharmapuri district, Tamil Nadu, India. *International Journal of Recent Scientific Research* **9**(1), 23306–23314. https:/dx.doi.org/10.24327/ijrsr.2018.0901.1442.

Trivedy, R. K. & Goel, P. K. 1986 Chemical and biological method for water pollution studies. *Environmental Publication (Karad, India)* **6**, 10–12.

Vijay, K. S. & Waman, S. N. 2015 Use of Strychnos Potatorum seed powder as a water purifier: A sustainable approach for rural development. *Global Journal for Research Analysis* **4**(7), 136–137.

Wang, L., Hu, C. & Shao, L. 2017 The antimicrobial activity of nanoparticles: Present situation and prospects for the future. *nternational Journal of Nanomedicine* **12**, 1227–1249.

First received 4 August 2023; accepted in revised form 8 February 2024. Available online 22 February 2024